Milan Krbálek

Analytical derivation of time spectral rigidity for thermodynamic traffic gas

Kybernetika, Vol. 46 (2010), No. 6, 1108--1121

Persistent URL: http://dml.cz/dmlcz/141470

KYBERNETIKA — VOLUME *46* (2010), NUMBER 6, PAGES 1108–1121

ANALYTICAL DERIVATION OF TIME SPECTRAL RIGIDITY FOR THERMODYNAMIC TRAFFIC GAS

Milan Krbálek

We introduce an one-dimensional thermodynamical particle model which is efficient in predictions about a microscopical structure of animal/human groups. For such a model we present analytical calculations leading to formulae for time clearance distribution as well as for time spectral rigidity. Furthermore, the results obtained are reformulated in terms of vehicular traffic theory and consecutively compared to experimental traffic data.

Keywords: thermodynamic traffic gas, clearance distribution, spectral rigidity

Classification: 82B21, 70F45, 37L99

1. INTRODUCTION

Movements of an arbitrary group of humans or animals show many common features originated from group dynamics ([3, 15], and [14]). For purposes of this article the animal/human groups are understood as a self-organized systems whose individual agents are influenced by other agents in the group (see for example [13]). It means that the agent adapts its behavior to the behavior of the rest of group. Such a influence is naturally restricted to the interactions with agents occurring in the close neighborhood (short-ranged interactions). Moreover, the decision-making process of the moving agent is influenced by the various factors (individuality of the agent, actual mental strain, control signals, information inflow, random factors and so on). Typically, the mediated collective decision-making of a group leads to effects of crowding, i. e. to the formation of congested states when the movement of one agent is strongly restricted by other agents. One of these effects is visualized in the Figure 1.

It is obvious that mutual interactions among the agents cause the changes in the system dynamics, which finally results in relevant changes of macroscopic quantities for the system investigated (see [6] and [4]). Furthermore, macroscopic relations describing the global behavior of transport systems influence significantly the microscopic structure of the system. Such a structure is, as understandable, of statistical nature, which is caused by the individuality of each agent. Whereas for free flow states one can detect the random distribution of the system elements, for congested states the strong psychological repulsion among crowding agents leads to the strong systemization of the ensemble (see [5, 7]). Recently, these microscopic phenomenons

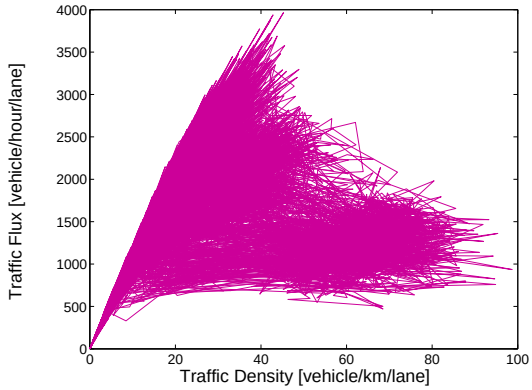

Fig. 1. Fundamental Diagram of Traffic Flow. Traffic flux J as a function of traffic density ϱ. The diagram is divided into three regions:
1. The free flow region (up to $\varrho \approx 30$) where cars move without any restrictions.
2. The region of metastable traffic ($30 \lessapprox \varrho \lessapprox 45$) where the heightened density causes the reinforcement of mutual interactions among vehicles.
3. The congested flow region ($\varrho \gtrapprox 45$) where the traffic is fully saturated and the movement of cars is therefore significantly restricted.

are measurable ([1, 11, 10]), which opens new possibilities to inspect a local behavior in animal/human groups.

The main goal of this article is to obtain meaningful predictions for the microstructure of traffic sample (similarly to [2] or [8]) and compare the results obtained to freeway measurements.

2. FORMULATION OF SOCIO-PHYSICAL TRANSPORT MODEL

Consider N identical particles (agents) on the unit sphere (see Figure 2)

$$S = \left\{ \vec{\xi} \in \mathbb{R}^3 : \|\vec{\xi}\|_{\mathsf{e}} = 1 \right\},$$

where the symbol $\|.\|_{\mathsf{e}}$ corresponds to the standard (euclidean) norm, i. e. $\|\vec{\xi}\|_{\mathsf{e}} = \sqrt{\xi_1^2 + \xi_2^2 + \xi_3^2}$. Let $\vec{x}_i = (\theta_i, \varphi_i)$ $(i = 1 \dots N)$ denote the position of the ith particle, where θ_i and φ_i represent the spherical angles (latitude and longitude) of standard spherical coordinates. Let $\vec{v}_i$ stand for the actual velocity of ith particle and parameter $\vec{v}_{\mathrm{d}}$ is the desired velocity (the same for all agents). Denoting the general metric in the system as $\|\vec{x} - \vec{y}\|$ one can define the $\varepsilon-$neighborhood of the particle i according to

$$O_\varepsilon^\star(\vec{x}_i) = \left\{ \vec{\xi} \in \mathbb{R}^3 : \ \xi_1^2 + \xi_2^2 + \xi_3^2 = 1 \ \wedge \ 0 < \|\vec{\xi} - \vec{x}_i\| < \varepsilon \right\}.$$

Thus, the indexing set

$$I_i = \left\{ k : \ \vec{x}_k \in O_\varepsilon^\star(\vec{x}_i) \right\}$$

cumulates all the particles being inside the $\varepsilon-$neighborhood of the ith particle. We remark that the general metric $\|\vec{x}-\vec{y}\|$ can be chosen arbitrary (with reference to the systems observed), but the most usual choice is the euclidean metric.

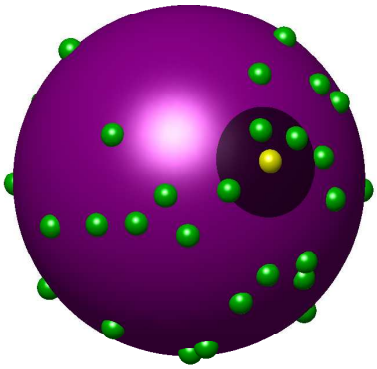

Fig. 2. Agents on the Unit Sphere. The selected agent (light) and his/her $\varepsilon-$neighborhood. The agent reacts only to the agents occurring in his/her $\varepsilon-$neighborhood $O_{\varepsilon}^{\star}$.

Aiming to quantify the mutual interactions among the agents we introduce the short-ranged potential energy

$$U \propto \sum_{i=1}^{N} \sum_{k \in I_i} V\left(r_{ik}\right),$$

where $V(r_i)$ corresponds to the repulsive two-body potential depending on the general distance $r_{ik} = \|\vec{x}_i - \vec{x}_k\|$ between the $\varepsilon-$neighboring particles only. The interaction of such a kind is chosen with the respect to the realistic behavior of animals/humans (see [7]). Besides, the potential $V(r)$ has to be defined so that $\lim_{r\to 0_+} V(r) = \infty$, which prevents particles from passing through each other. The socio-physical hamiltonian of the described ensemble reads as

$$\mathcal{H}_{\varepsilon} = \frac{m}{2} \sum_{i=1}^{N} \|\vec{v}_i - \vec{v}_{\mathrm{d}}\|_{\mathsf{e}}^2 + c \sum_{i=1}^{N} \sum_{k \in I_i} V\left(r_{ik}\right),$$

where m represents a mass of particles and c is a calibrating coefficient. Whereas the second summand in the previous formula describes the particle attraction/repulsion the former takes into account the fact that driver moving with the desired velocity does not accelerate/decelerate (if not fettered by the other cars).

The above-mentioned description is strictly deterministic and does not reflect the statistical features of realistic human/animal communities. Therefore we introduce a thermodynamical alternative of the model (see [5] or [18]) where the entire system

is exposed (if using the thermodynamical terminology) to a "heat bath" of a given temperature T, i.e. to random influences of a certain variance and statistics. Denote

$$\beta = (\mathrm{k}T)^{-1}$$

where k is the Boltzmann constant. The thermal parameter β can be interpreted as a psychological coefficient describing a level of the mental pressure under the driver is while driving his/her car. Hence, in the next part of this article we call β as a mental strain coefficient.

Implementing this thermal component into the originally deterministic system we have obtained the statistical ensemble whose thermal equilibrium is described statistically. It means that the microscopical quantities (gaps among the cars, velocities of single vehicles, time intervals among the subsequent cars and so on) measured in thermal equilibrium are determined by means of corresponding probability densities. This fact fully corresponds to the ascertainments observed by the traffic experiments (see [19] and [16]).

3. CIRCULAR VARIANT OF THE MODEL

Restricting the particle movement to the circular curve

$$C = \left\{ \vec{\xi} \in \mathbb{R}^2 : \|\vec{\xi}\|_{\mathtt{e}} = 1 \right\}$$

the previous thermal scheme converts to the simple model of one-lane traffic. In this case the location of each particle is unambiguously described by its angular coordinate φ_i. Then the hamiltonian of this one-dimensional system reads as

$$\mathcal{H} = \frac{m}{2} \sum_{i=1}^{N} (v_i - v_{\mathrm{d}})^2 + c \sum_{i=1}^{N} V(r_i),$$

where

$$r_i := |\varphi_{i+1} - \varphi_i| \frac{N}{2\pi}$$

corresponds to the re-scaled circular distance between $(i+1)$th and ith particles. Denoting $\varphi_{N+1} = \varphi_1$ for convenience the following equality holds true

$$\sum_{i=1}^{N} r_i = N. \tag{1}$$

As published in [9] the suitable choice for two-body traffic potential is the power-law function $V(r) = r^{-1}$. Under these conditions the corresponding partition function is of a form

$$\mathcal{Z} = \int_{\mathbb{R}^{2N}} \delta \left(N - \sum_{i=1}^{N} r_i \right) \prod_{i=1}^{N} \mathtt{e}^{-\frac{m}{2}\beta(v_i - v_{\mathrm{d}})^2} \ \mathtt{e}^{-\frac{\beta}{r_i}} \mathtt{d}r_1 \ldots \mathtt{d}r_N \mathtt{d}v_1 \ldots \mathtt{d}v_N. \tag{2}$$

Here $\delta(x)$ stands for the Dirac $\delta-$function. After $2N-1$ integrations we find out that individual velocity v of particles is Gaussian distributed, i. e.

$$q(v) = \frac{1}{\sqrt{2\pi}\sigma}\ \mathtt{e}^{-\frac{(v-v_{\mathrm{d}})^2}{2\sigma^2}} \tag{3}$$

is the corresponding probability density, where $\sigma^{-1} = \sqrt{m\beta}$. Similarly, denoting by $\Theta(x)$ the Heaviside's step function

$$\Theta(x) = \begin{cases} 1, & x > 0 \\ 0, & x \leqslant 0 \end{cases}$$

and by $\mathcal{K}_\lambda(x)$ the modified Bessel's function of the second kind (the Mac-Donald's function) there has been derived in the article [9] that probability density for gap among the succeeding cars (clearance distribution) reads as

$$\wp(r) = A\ \Theta(r)\ \mathtt{e}^{-\frac{\beta}{r}}\mathtt{e}^{-Br}, \tag{4}$$

where

$$B = \beta + \frac{3-\mathtt{e}^{-\sqrt{\beta}}}{2}, \tag{5}$$

$$A^{-1} = 2\sqrt{\frac{\beta}{B}}\mathcal{K}_1\big(2\sqrt{B\beta}\big). \tag{6}$$

We remark that $\wp(r)$ fulfils two normalization conditions

$$\int_{\mathbb{R}} \wp(r)\ \mathtt{d}r = 1 \tag{7}$$

and

$$\int_{\mathbb{R}} r\ \wp(r)\ \mathtt{d}r = 1. \tag{8}$$

The latter represents a scaling to a mean clearance equal to one. The distribution (4) is in a good agreement with the clearance distribution observed in the real-road data (see [7, 9, 10], and [17]). We add that the inverse temperature β of the real traffic ensemble is related to the traffic density ϱ.

4. DERIVATION OF TIME CLEARANCE DISTRIBUTION

Although the distance clearance distribution of traffic sample can be actually very well estimated by the formula (4) the direct measurement of traffic clearances is less usual. Since the majority of experimental data is measured by the induction-loop detectors the clearances are calculated vicariously by means of velocities and time clearances. Such a method brings an additional vagueness into a distance clearance statistics (predominantly in the congested traffic area).

A natural way how to eliminate such a drawback can be found in analytical derivation of suitable estimations for time clearance. i. e. for probability density of

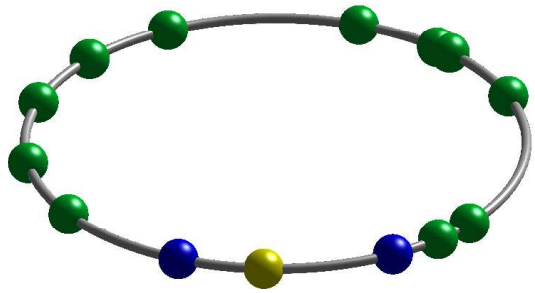

Fig. 3. Vehicles on the Unit Circle. The interaction among the agents (drivers) is strictly short-ranged, which means that the particle (light) interacts with two neighbors only.

netto time gaps among all pairs of subsequent cars. The intended analytical calculations will be introduced in the following text. Knowing the velocity distribution $q(v)$ and distance clearance distribution $\wp(r)$ one can trivially deduce that time headway distribution reads as

$$\tau(t) = \int_{\mathbb{R}} vq(v)\wp(vt)\,\mathtt{d}v.$$

After denoting $f(v) = v\wp(vt)$ we expand such a function into the Taylor's series about the optimal velocity v_{d}. Thus

$$f(v) = f(v_{\mathrm{d}}) + \sum_{\ell=1}^{\infty} \frac{\mathtt{d}^{\ell} f}{\mathtt{d}v^{\ell}}(v_{\mathrm{d}}) \frac{(v - v_{\mathrm{d}})^{\ell}}{\ell!},$$

where

$$\frac{\mathtt{d}^{\ell} f}{\mathtt{d}v^{\ell}} = \frac{\partial^{\ell}\wp}{\partial(vt)^{\ell}} t^{\ell} v + \ell \frac{\partial^{\ell-1}\wp}{\partial(vt)^{\ell-1}} t^{\ell-1} \quad (\ell \in \mathbb{N}).$$

Hence

$$\begin{aligned}\tau(t) = v_{\mathrm{d}}\wp(v_{\mathrm{d}}t) &+ \sum_{\ell=1}^{\infty} \frac{1}{\ell!} \frac{\partial^{\ell}\wp}{\partial(vt)^{\ell}}(v_{\mathrm{d}}t) t^{\ell} v_{\mathrm{d}} \int_{\mathbb{R}} (v - v_{\mathrm{d}})^{\ell} q(v)\ \mathtt{d}v \\ &+ \sum_{\ell=1}^{\infty} \frac{1}{\ell!} \frac{\partial^{\ell-1}\wp}{\partial(vt)^{\ell-1}}(v_{\mathrm{d}}t) t^{\ell-1} \int_{\mathbb{R}} (v - v_{\mathrm{d}})^{\ell} q(v)\ \mathtt{d}v \\ &= v_{\mathrm{d}}\wp(v_{\mathrm{d}}t) + \sum_{\ell=1}^{\infty} \frac{\mu_{\ell}}{\ell!} \left(\frac{\partial^{\ell}\wp}{\partial(vt)^{\ell}}(v_{\mathrm{d}}t) t^{\ell} v_{\mathrm{d}} + \frac{\partial^{\ell-1}\wp}{\partial(vt)^{\ell-1}}(v_{\mathrm{d}}t) t^{\ell-1} \right),\end{aligned}$$

where $\mu_{\ell} = \int_{\mathbb{R}} (v - v_{\mathrm{d}})^{\ell} q(v)\,\mathtt{d}v$ is $\ell-$th statistical moment with three prerogatived cases $\mu_0 = 1$, $\mu_1 = 0$, and $\mu_2 = \sigma^2$. The latter represents a statistical variance (see

also (3)). Using this knowledge one can effortlessly find a following approximation for time clearance distribution

$$\tau(t) \approx v_{\mathrm{d}} \wp(v_{\mathrm{d}} t) + \frac{\sigma^2}{2} \left(\frac{\partial^2 \wp}{\partial (vt)^2}(v_{\mathrm{d}} t) t^2 v_{\mathrm{d}} + 2 \frac{\partial \wp}{\partial (vt)}(v_{\mathrm{d}} t) t \right). \tag{9}$$

Owing to the facts that

$$\int_{\mathbb{R}} \left(\frac{\partial^2 \wp}{\partial (vt)^2}(v_{\mathrm{d}} t) t^2 v_{\mathrm{d}} + 2 \frac{\partial \wp}{\partial (vt)}(v_{\mathrm{d}} t) t \right) \mathtt{d}t = 0$$

and the variance is decreasing function of inverse temperature β we operate (in the next part of the text) with the approximation formula

$$\tau(t) = A\ \Theta(t)\ \mathtt{e}^{-\frac{\beta}{t}} \mathtt{e}^{-Bt} =: \tau_\beta(t), \tag{10}$$

where the relations (5), (6) hold true. Again, we use the normalization and re-scaling conditions like

$$\int_{\mathbb{R}} \tau(t)\, \mathtt{d}t = \int_{\mathbb{R}} t\, \tau(t)\, \mathtt{d}t = 1.$$

5. DERIVATION OF TIME SPECTRAL RIGIDITY

Description of traffic microstructure by means of inter-vehicle time gap distribution $\tau(t)$ is, as discussed above, more appropriate than inter-vehicle distance gap distribution. However, both of them depict the time/distance gaps between two successive vehicles only. Aiming to investigate the middle-ranged interactions among the cars it is necessary to find a mathematical quantity suitable for quantifying the level of synchronization for larger clusters of particles. This desired quantity can be found in Random Matrix Theory (see [12]) where it provides the insight into the structure of eigenvalues of random matrix ensembles. It is called *a spectral rigidity.* If reformulated within the bounds of traffic theory *the time spectral rigidity* has the following interpretation.

Consider a set $\{t_i : i = 1 \dots Q\}$ of netto time gaps between each pair of the subsequent cars moving in the same lane. We suppose that the mean time gap taken over the complete set is re-scaled to one, i. e.

$$\sum_{i=1}^{Q} t_i = Q.$$

Dividing the time interval $[0, Q)$ into subintervals $\big[(k-1)T, kT\big)$ of a length T and denoting by $n_k(T)$ the number of cars in the $k-$th subinterval, the average value $\overline{n}(T)$ taken over all possible subintervals is

$$\overline{n}(T) = \frac{1}{\lfloor Q/T \rfloor} \sum_{k=1}^{\lfloor Q/T \rfloor} n_k(T) = T,$$

where the integer part $\lfloor Q/T \rfloor$ stands for the number of all subintervals $\big[(k-1)T, kT\big)$ included in the entire interval $[0, Q)$. We suppose, for convenience, that Q/T is integer, i. e. $\lfloor Q/T \rfloor = Q/T$. The time spectral rigidity $\Delta(T)$ is then defined as

$$\Delta(T) = \frac{T}{Q} \sum_{k=1}^{Q/T} \big(n_k(T) - T\big)^2$$

and represents the statistical variance of the number of vehicles passing a given fixed point of the road during the time interval T.

Knowing the one parameter family of the probability densities (10) we can derive an analytical prediction for the rigidity $\Delta(T)$ of the related thermodynamical traffic gas. Let $\tau_n(t)$ represent the nth nearest-neighbor probability density, i.e. the probability density for the time gap t between the $n+2$ neighboring particles. Using this notation we find that the probability density for the gap between two succeeding particles (cars) is $\wp(t) = \wp_0(t)$. Regarding the spacings as independent the nth probability density $\tau_n(t)$ can be calculated via recurrent formula

$$\tau_n(t) = \tau_{n-1}(t) \ \star \ \tau_0(t),$$

where symbol $\star$ represents a convolution of the two probabilities, i.e.

$$\tau_n(t) = \int_{\mathbb{R}} \tau_{n-1}(s)\tau_0(t-s)\,\mathtt{d}s.$$

Using the method of mathematical induction and an approximation of the function

$$g_n(t,s) = \mathtt{e}^{-\beta\left(\frac{n^2}{s} + \frac{1}{t-s}\right)} \approx \mathtt{e}^{-\frac{\beta}{t}(n+1)^2}$$

in the saddle point one can obtain

$$\tau_n(t) = \Theta(t) \int_0^t N_{n-1}N_0 s^{n-1} \mathtt{e}^{-\beta\frac{n^2}{s}} \mathtt{e}^{-Bs} \mathtt{e}^{-\frac{\beta}{t-s}} \mathtt{e}^{-B(t-s)}\,\mathtt{d}s =$$

$$= \Theta(t) N_{n-1}N_0 \mathtt{e}^{-Bt} \int_0^t s^{n-1} g_n(t,s)\,\mathtt{d}s \approx$$

$$\approx \Theta(t) N_{n-1}N_0 \mathtt{e}^{-\frac{\beta}{t}(n+1)^2} \mathtt{e}^{-Bt} \int_0^t s^{n-1}\,\mathtt{d}s \approx \Theta(t) N_{n-1}N_0 n^{-1} t^n \mathtt{e}^{-\frac{\beta}{t}(n+1)^2} \mathtt{e}^{-Bt}.$$

Hence

$$\tau_n(t) \approx \Theta(t) N_n t^n \mathtt{e}^{-\frac{\beta}{t}(n+1)^2} \ \mathtt{e}^{-Bt}$$

where (after applying the re-normalization procedure)

$$N_n^{-1} = 2\left(\sqrt{\frac{\beta}{B}}(n+1)\right)^{n+1} \mathcal{K}_{n+1}\big(2(n+1)\sqrt{B\beta}\big).$$

This fixes the proper normalization $\int_{\mathbb{R}} \tau_n(t)\,\mathtt{d}t = 1$. In addition to that the mean spacing equals to

$$\int_{\mathbb{R}} t\tau_n(t)\,\mathtt{d}t = n+1.$$

According to [12] the variance $\Delta(T)$ could be evaluated by the formula

$$\Delta(T) = T - 2\int_0^T (T-t)\big(1-R(t)\big)\,\mathtt{d}t, \tag{11}$$

where

$$R(t) = \sum_{n=0}^{\infty} \tau_n(t)$$

is the *two-point cluster function.* A convenient way to calculate the asymptotic behavior of the variance $\Delta(T)$ for large T is the application of the Laplace transformation to the two-point cluster function, i. e. $y(\eta) = \int_{\mathbb{R}} R(t)\ \mathtt{e}^{-\eta t}\,\mathtt{d}t$. It leads to a partial result

$$y(\eta) = \sum_{n=0}^{\infty} \left(\frac{B}{B+\eta}\right)^{\frac{n+1}{2}} \frac{\mathcal{K}_{n+1}\big(2(n+1)\sqrt{(B+\eta)\beta}\big)}{\mathcal{K}_{n+1}\big(2(n+1)\sqrt{B\beta}\big)}.$$

The asymptotic behavior of the Mac-Donald's function

$$\mathcal{K}_n(x) \approx \frac{2^{n-1}\Gamma(n)}{x^n}\ \mathtt{e}^{-x} \qquad (x \ll 1)$$

(where $\Gamma(x)$ represents the gamma-function) provides the approximation

$$y(\eta) \approx \left(\frac{B+\eta}{B}\ \frac{\mathtt{e}^{2\sqrt{(B+\eta)\beta}}}{\mathtt{e}^{2\sqrt{B\beta}}} - 1\right)^{-1}.$$

Applying the Maclaurin's expansion (Taylor's expansion about the point zero) of the function $h(\eta) = \eta \cdot y(\eta)$ to order η^2 we obtain

$$y(\eta) \approx \frac{1}{\eta} + \alpha_0 + \alpha_1\eta + \mathcal{O}(\eta^2),$$

where

$$\alpha_0 = -\frac{2B\beta + 3\sqrt{B\beta}}{4\big(1+\sqrt{B\beta}\big)^2},$$

$$\alpha_1 = \frac{6\sqrt{B\beta} + B\beta\big(21 + 4B\beta + 16\sqrt{B\beta}\big)}{48B\big(1+2\sqrt{B\beta}\big)^3}.$$

With the help of the equation (11) and the inverse Laplace transform

$$R(t) = \frac{1}{2\pi\mathtt{i}} \lim_{\varphi\to\infty} \int_{c-\mathtt{i}\varphi}^{c+\mathtt{i}\varphi} y(\eta)\mathtt{e}^{\eta t}\,\mathtt{d}\eta$$

then we get finally

$$\Delta(T) = \chi T + \gamma + \mathcal{O}(T^{-1}), \tag{12}$$

where

$$\chi = \chi(\beta) = \frac{2 + \sqrt{B\beta}}{2B(1 + \sqrt{B\beta})} \tag{13}$$

and

$$\gamma = \gamma(\beta) = \frac{6\sqrt{B\beta} + B\beta\big(21 + 4B\beta + 16\sqrt{B\beta}\big)}{24\big(1 + \sqrt{B\beta}\big)^4}. \tag{14}$$

We finalize these mathematical calculations by the assertion that the time spectral rigidity displays a linear dependence (12) for large time intervals T.

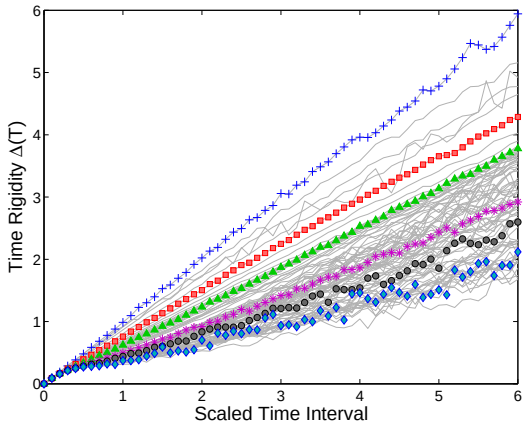

Fig. 4. Time Spectral Rigidity. Gray curves correspond to the time rigidity $\Delta(T)$ analyzed separately in 85 density regions. The chosen results of relevant statistical analysis are picked out. Concretely, blue plus signs, red squares, green triangles, magenta stars, black circles, and turquoise diamonds represent the rigidities obtained for traffic data from the following density regions: [2,3); [6,7); [16,17); [26,27); [40,41); and [85,86) vehicles/km/lane respectively.

6. STATISTICAL ANALYSIS OF TRAFFIC DATA

Single-vehicle data investigated for purposes of this article were measured continuously during three months on the Netherlands two-lane freeway A9. Macroscopic traffic density ϱ was calculated for samples of $N = 50$ subsequent cars passing a double-induction-loop detector. For the intentions outlined above we divide the region of the measured densities $\varrho \in [0, 85$ veh/km/lane] into 85 equidistant subintervals and separately analyze the data from each one of them. The sketched procedure prevents the undesired mixing of the states with the different inverse temperature β, i. e. with the different psychological strain of drivers. Netto time distances t_i among the succeeding cars (ith and $(i-1)$th) were calculated directly from the data after eliminating car-truck, truck-car, and truck-truck gaps.

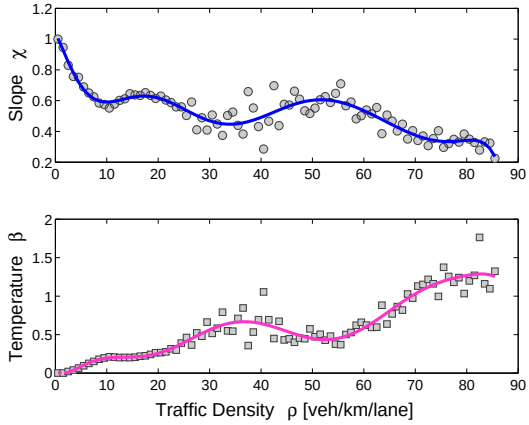

Fig. 5. Slope of Spectral Rigidity and Inverse Temperature. The circles in the upper subplot display the slope of the spectral rigidity $\Delta(T)$ (see Figure 4), separately evaluated for the various traffic densities. The lower subplot visualizes the corresponding values of the inverse temperature β. The continuous curves represent a polynomial approximations of the relevant data.

As unambiguously followed from the robust statistical analysis the time clearance distribution of freeway traffic data corresponds to the theoretical prediction $\tau_\beta(t)$ very well. The chosen representative of the relevant analysis are displayed in the Figure 6. Here one can detect the basic probabilistic trends of time gaps among succeeding cars. Whereas in the region of small densities (free traffic regime) the relevant probability density is exponential essentially (which fully corresponds to the fact that cars interactions are negligible) the distribution $\tau(t)$ is rapidly changing if congested data are observed. In this case the strong mutual interactions among vehicles lead to the hardcore repulsions in the system which results in fact that

$$\lim_{t\to 0_+} \tau(t) = 0.$$

Furthermore, the time spectral rigidity of traffic samples has been investigated. As shown in the Figure 4 the theoretical properties of the function $\Delta(T)$ agree with the behavior of the rigidity evaluated from the traffic data. The comparison with formula (12) allows us to determine the empirical dependence of the inverse temperature β on the traffic density ϱ. The results of such a analysis are visualized in the Figure 5. Such a dependence (plotted at the bottom of the Figure 5) shows a virtually linear increase in the region of free traffic (up to $\varrho \approx 20$ veh/km/lane) with a visible plato for densities around 12 veh/km/lane. For saturated traffic states, where $\varrho \gtrapprox 50$ veh/km/lane, one can similarly observe almost linear increase of temperature β with density ϱ. The intermediate region of metastable traffic states shows a substantial growth of temperature. This is influenced by the fact that driver, moving quite fast in relatively dense traffic flow, is under a considerable psychological pressure. After the transition from free to congested regime (between

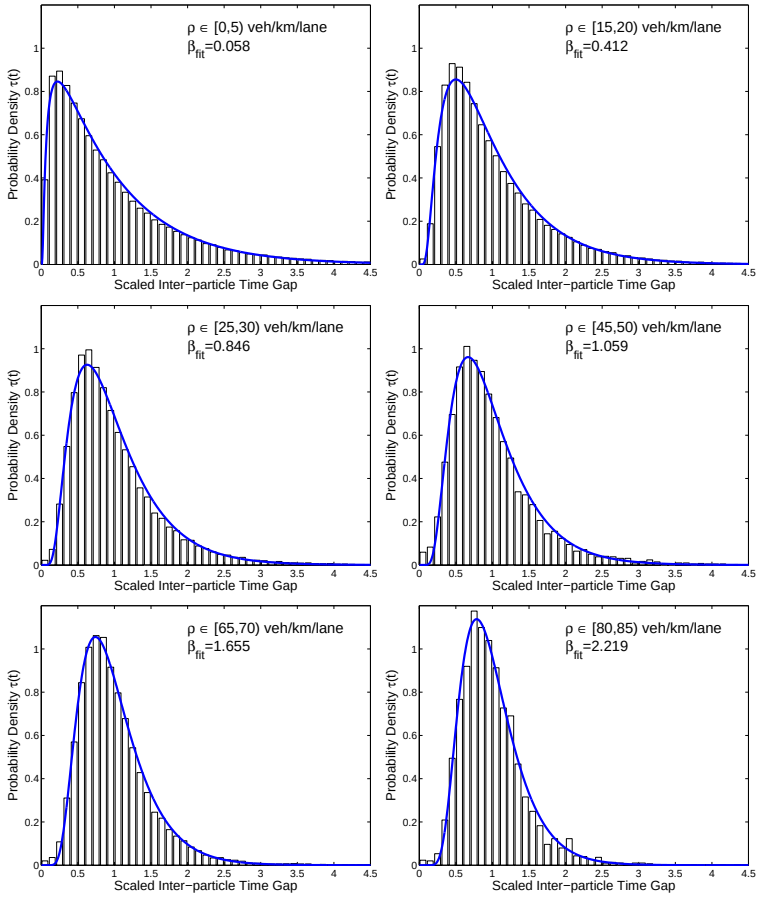

Fig. 6. Time Headway Distribution. The bars represent the inter-particle time gaps measured among the subsequent vehicles moving on the freeway. The entire data file has been divided into small density regions (see legend for details) to separate the different traffic regimes. The blue curves display the predictions of our theory for fitted value of inverse temperature β. Optimal value of β_{fit} was obtained by minimizing the χ^2-statistics.

40 and 50 veh/km/lane), the pressure continues to decline because of decrease in mean velocity. Finally, if the traffic flow become denser and denser the mental strain coefficient β is increasing further. It finally culminates by the creation of stop-and-go traffic waves. It is evident that the empirical relation $\beta = \beta(\varrho)$ between the strain coefficient β and traffic density ϱ fully corresponds to intuitive substance of traffic reality.

7. CONCLUSION

We have presented calculations leading to the analytical formula for netto time gap among the subsequent particle of thermodynamic traffic gas. The calculated prediction has been successfully compared to the vehicular traffic data measured by loop detectors. Furthermore, we have introduced the mathematical procedure leading to the formula for time spectral rigidity describing mutual interaction of the more extensive clusters of succeeding cars. Analytical predictions obtained by means of such a procedure has been confronted to the results of relevant statistical analyzes. Beyond all doubt it has been ascertained that time spectral rigidity shows a predicted linear dependence on the length of time interval. Such a correspondence leads to the vicarious detection of the thermal parameter β quantifying the mental strain of cars drivers during their driving manoeuvres.

ACKNOWLEDGEMENT

This work was supported by the Ministry of Education, Youth and Sports of the Czech Republic within the projects LC06002 and MSM 6840770039.

(Received July 2, 2010)

REFERENCES

[1] C. Appert-Rolland: Experimental study of short-range interactions in vehicular traffic. Phys. Rev. E *80* (2009), 036102(1)–036102(5).

[2] J. Baik, A. Borodin, P. Deift, and T. Suidan: A model for the bus system in Cuernavaca (Mexico). J. Phys. A: Math. Gen. *39* (2006), 8965–8975.

[3] A. L. Barabási: The origin of bursts and heavy tails in human dynamics. Nature (London) *435* (2005), 207–211.

[4] D. Helbing: Traffic and related self-driven many-particle systems. Rev. Mod. Phys. *73* (2001), 1067–1141.

[5] D. Helbing, M. Treiber, and A. Kesting: Understanding interarrival and interdeparture time statistics from interactions in queuing systems. Physica A *363* (2006), 62–72.

[6] D. Chowdhury, L. Santen, and A. Schadschneider: Statistical Physics of Vehicular Traffic and Some Related Systems. Physics Reports *329* (2000), 199–369.

[7] M. Krbálek and D. Helbing: Determination of interaction potentials in freeway traffic from steady-state statistics. Physica A *333* (2004), 370–378.

[8] D. Jezbera, D. Kordek, J. Kříž, P. Šeba, and P. Šroll: Walkers on the circle. J. Stat. Mech. (2010), L01001(1)–L01001(6).

[9] M. Krbálek: Equilibrium distributions in a thermodynamical traffic gas. J. Phys. A: Math. Theor. *40* (2007), 5813–5821.

[10] M. Krbálek: Inter-vehicle gap statistics on signal-controlled crossroads. J. Phys. A: Math. Theor. *41* (2008), 205004(1)–205004(8).

[11] M. Krbálek and P. Šeba: Spectral rigidity of vehicular streams (random matrix theory approach). J. Phys. A: Math. Theor. *42* (2009), 345001(1)–345001(10).

[12] M. L. Mehta: Random Matrices (revised and enlarged). Academic Press, New York 1991.

[13] H. Moon, D. E. Conlon, S. E. Humphrey, N. Quigley, C. E. Devers, and J. M. Nowakowski: Group decision process and incrementalism in organizational decision making. Organizational Behavior and Human Decision Processes *92* (2003), 67–79.

[14] J. G. Oliveira and A. L. Barabási: Human dynamics: Darwin and Einstein correspondence patterns. Nature (London) *437* (2005), 1251–1253.

[15] J. G. Oliveira and A. Vazquez: Impact of interactions on human dynamics. Physica A *388* (2009), 187–192.

[16] G. Orosz, R. E. Wilson, R. Szalai, and G. Stépán: Exciting traffic jams: Nonlinear phenomena behind traffic jam formation on highways. Phys. Rev. E *80* (2009), 046205(1)–046205(12).

[17] D. Smith, J. Marklof, and R. E. Wilson: Improved power law potentials for highway traffic flow. Submitted to Eur. Phys. J. B (2008), *preprint* http://rose.bris.ac.uk/dspace/bitstream/1983/1061/1/dasmith.pdf.

[18] A. Sopasakis: Stochastic noise approach to traffic flow modeling. Physica A *342* (2004), 741–754.

[19] Y. Sugiyama, M. Fukui, M. Kikuchi, K. Hasebe, A. Nakayama, K. Nishinari, S. Tadaki, and S. Yukawa: Traffic jams without bottlenecks–experimental evidence for the physical mechanism of the formation of a jam. New Journal of Physics, *10* (2008), 033001(1)–033001(8).

Milan Krbálek, Faculty of Nuclear Sciences and Physical Engineering, Czech Technical University in Prague, Trojanova 13, 120 00 Praha. Czech Republic.

e-mail: milan.krbalek@fjfi.cvut.cz